Neutralization of Osteopontin Inhibits Obesity-Induced Inflammation and Insulin Resistance

Florian W. Kiefer,[1] Maximilian Zeyda,[1] Karina Gollinger,[1] Birgit Pfau,[1] Angelika Neuhofer,[1] Thomas Weichhart,[2] Marcus D. Säemann,[2] René Geyeregger,[1] Michaela Schlederer,[3] Lukas Kenner,[3,4] and Thomas M. Stulnig[1]

OBJECTIVE—Obesity is associated with a state of chronic low-grade inflammation mediated by immune cells that are primarily located to adipose tissue and liver. The chronic inflammatory response appears to underlie obesity-induced metabolic deterioration including insulin resistance and type 2 diabetes. Osteopontin (OPN) is an inflammatory cytokine, the expression of which is strongly upregulated in adipose tissue and liver upon obesity. Here, we studied OPN effects in obesity-induced inflammation and insulin resistance by targeting OPN action in vivo.

RESEARCH DESIGN AND METHODS—C57BL/6J mice were fed a high-fat diet to induce obesity and were then intravenously treated with an OPN-neutralizing or control antibody. Insulin sensitivity and inflammatory alterations in adipose tissue and liver were assessed.

RESULTS—Interference with OPN action by a neutralizing antibody for 5 days significantly improved insulin sensitivity in diet-induced obese mice. Anti-OPN treatment attenuated liver and adipose tissue macrophage infiltration and inflammatory gene expression by increasing macrophage apoptosis and significantly reducing c-Jun NH_2-terminal kinase activation. Moreover, we report OPN as a novel negative regulator for the activation of hepatic signal transducer and activator of transcription 3 (STAT3), which is essential for glucose homeostasis and insulin sensitivity. Consequently, OPN neutralization decreased expression of hepatic gluconeogenic markers, which are targets of STAT3-mediated downregulation.

CONCLUSIONS—These findings demonstrate that antibody-mediated neutralization of OPN action significantly reduces insulin resistance in obesity. OPN neutralization partially decreases obesity-associated inflammation in adipose tissue and liver and reverses signal transduction related to insulin resistance and glucose homeostasis. Hence, targeting OPN could provide a novel approach for the treatment of obesity-related metabolic disorders. ***Diabetes*** **59:935–946, 2010**

From the [1]Clinical Division of Endocrinology and Metabolism, Department of Medicine III, Medical University of Vienna, Vienna, Austria; the [2]Clinical Division of Nephrology and Dialysis, Department of Medicine III, Medical University of Vienna, Vienna, Austria; the [3]Ludwig Boltzmann Institute for Cancer Research, Medical University of Vienna, Vienna, Austria; and the [4]Department of Pathology, Medical University of Vienna, Vienna, Austria.

Corresponding author: Thomas M. Stulnig, thomas.stulnig@meduniwien.ac.at.

Received 17 March 2009 and accepted 17 January 2010. Published ahead of print at http://diabetes.diabetesjournals.org on 27 January 2010. DOI: 10.2337/db09-0404.

Obesity is a major risk factor for the development of insulin resistance, which is a fundamental step toward type 2 diabetes and cardiovascular disease (1). The chronic low-grade inflammation associated with obesity as determined by increased systemic concentrations of inflammatory markers and cytokines in patients and animal models of obesity (2) probably represents a crucial link between obesity and insulin resistance (3). This systemic inflammatory response primarily originates from adipose tissue and liver (4). Both tissues produce a variety of inflammatory proteins such as interleukin (IL)-1β, IL-6, tumor necrosis factor (TNF)-α, monocyte chemoattractant protein (MCP)-1, and C-reactive protein (CRP). The serum concentrations of all of these mediators are elevated in obesity (2,5). Within the adipose tissue, inflammatory adipokines are predominantly derived from nonfat cells such as macrophages (6,7). The abundance of adipose tissue macrophages is markedly increased in obese patients and rodent models of obesity (6,8,9). Both, adipose tissue and the liver have an architectural organization in which metabolic cells (adipocytes and hepatocytes, respectively) are in close proximity to immune cells (adipose tissue macrophages and Kupffer cells, respectively), while both have immediate access to the vasculature. This tissue architecture allows continuous interactions between immune and metabolic responses (4).

Osteopontin (OPN; gene *Spp1*), also named secreted phosphoprotein-1 and sialoprotein-1, is a multifunctional protein expressed in activated macrophages and T-cells, osteoclasts, hepatocytes, smooth muscle, endothelial, and epithelial cells (10,11). OPN was originally classified as a T helper type 1 (Th1) cytokine that is involved in physiological and pathological mineralization in bone and kidney, cell survival, inflammation, and tumor biology (10,12). OPN induces the expression of a variety of proinflammatory cytokines and chemokines in peripheral blood mononuclear cells (13). Moreover, it functions in cell migration, particularly of monocytes/macrophages (11), and stimulates expression of matrix metalloproteases to induce matrix degradation and facilitate cell motility (14). Notably, OPN plays a role in various inflammatory disorders, such as rheumatoid arthritis (15) and atherosclerosis (16), in diabetic macro- and microvascular diseases (17), and hepatic inflammation (18). Hepatic OPN expression is upregulated in obesity (19) and in various models of liver injury where OPN is localized to macrophages and Kupffer cells (20,21). Furthermore, OPN is involved in the pathogenesis of nonalcoholic fatty liver disease (NAFLD), which is strongly associated with visceral obesity (19,22,23).

As reported recently, OPN gene expression is extensively upregulated upon obesity in human and murine

adipose tissue (24–26). While OPN plasma concentrations are elevated in morbidly obese patients, data are inconsistent in different murine models of obesity (24–27). A recent publication (26) provided evidence that genetic OPN deficiency improves diet-induced insulin resistance.

Therefore, we hypothesized that targeting OPN in established obesity could reverse obesity-associated adipose tissue inflammation and hepatic alterations and, consequently, insulin resistance. We show that antibody-mediated neutralization of OPN rapidly improved insulin sensitivity in obese mice. Macrophage accumulation in adipose tissue was considerably decreased and adipose tissue inflammation was partially attenuated in anti-OPN–treated mice. OPN neutralization increased hepatic signal transducer and activator of transcription 3 (STAT3) activation that crucially contributes to insulin sensitivity and downregulated genes related to hepatic inflammation and gluconeogenesis. Hence, neutralization of OPN action could provide a novel therapeutic approach for prevention and treatment of obesity-induced insulin resistance and type 2 diabetes.

RESEARCH DESIGN AND METHODS

Animals and diets. C57BL/6J mice were purchased from Charles River Laboratories (Sulzfeld, Germany). At 7 weeks of age, male littermates were placed for 24 weeks on a high-fat diet (HF group, n = 8/group, 60 kcal% fat, D12492; Research Diets, New Brunswisk, NJ) and normal chow diet (NC group, n = 5/group) to induce obesity and to serve as lean controls, respectively. All mice were housed in specific pathogen-free facility that maintained a 12-h light/dark cycle. Mice had free access to food and water, and food intake was monitored. Blood was drawn after 3 h fasting immediately before mice were killed. Gonadal white adipose tissue (GWAT) pads and liver were collected. The protocol was approved by the local ethics committee for animal studies and followed the guidelines on accommodation and care of animals formulated by the European Convention for the Protection of Vertebrate Animals Used for Experimental and Other Scientific Purposes.

Antibody treatment. Mice were treated with a neutralizing anti-mouse OPN IgG (50 μg/mouse) or control goat IgG three times during 5e days by tail-vein injection. OPN-specific IgG (R&D Systems, Minneapolis, MN) was produced in goats by immunizing with NSO-derived, recombinant mouse OPN. Mice were killed 2 days after last antibody application.

Metabolic measurements. Plasma glucose, cholesterol, triglyceride, and free fatty acid concentrations were measured in EDTA plasma by an automated analyzer (Falcor 350; A. Menarini Diagnostics, Florence, Italy). We used commercially available enzyme-linked immunosorbent assay kits to determine plasma insulin (Mercodia, Uppsala, Sweden), IL-6, TNF-α, leptin, adiponectin, OPN (all R&D Systems), and serum amyloid P (SAP) (Alpco Diagnostics, Windham, NH). Plasma concentrations of alanine aminotransferase (ALT) and aspartate aminotransferase (AST) were measured using the Reflotron analysis system (Roche, Mannheim, Germany). We calculated homeostasis model assessment of insulin resistance (HOMA-IR) as an index for insulin resistance (28). Insulin sensitivity was assessed by insulin tolerance test (ITT) after a 3-h fasting period. Blood glucose concentrations were measured before and 30, 60, 90, and 120 min after an intraperitoneal injection of recombinant human insulin (0.75 units/kg body wt Actrapid for HF and 0.25 units/kg for NC mice, respectively; Novo Nordisk, Bagsværd, Denmark). Glucose tolerance was assessed by a glucose tolerance test (GTT) after overnight fasting. Blood glucose concentrations were measured before and 30, 60, and 90 min after an intraperitoneal injection of 20% glucose (0.75 g/kg body wt for HF and 1.0 g/kg body wt for NC mice, respectively).

Immunoflourescence, immunohistochemistry, tunel staining, and flow cytometry. Frozen sections were prepared from murine GWAT and liver. Sections were stained with rat anti-mouse F4/80 and Mac-2 IgG antibodies (Serotec, Oxford, U.K. and Cedarlane, Burlington, ON, Canada, respectively). Primary antibodies were detected with AlexaFluor 488 or AlexaFluor 594 goat anti-rat IgG antibodies (Molecular Probes, Eugene, OR). As a negative control, isotype control staining was done on selected sections. Nuclei were visualized by DAPI staining. Slides were mounted in Vectashield (Vector Laboratories, Burlingame, CA) and examined under a fluorescence microscope (Leica, Wetzlar, Germany). Macrophage infiltration in adipose tissue and liver was quantified by calculating the ratio of F4/80- and Mac-2–positive cells to total nuclei (29). Apoptotic cells were stained on frozen sections using the Fluorescin In Situ Cell Dection Kit from Roche, according to manufacturer's instructions, in parallel with double staining for F4/80 and Mac-2, respectively, as described above.

For paraffin sections, GWAT and liver samples were fixed with neutral buffered 4% paraformaldehyde and were paraffin-embedded. Hematoxylin and eosin staining was performed in liver as described elsewhere (22). After dewaxation and rehydration, immunohistochemical staining for Mac-2 (Serotec) and pSTAT3 (Tyr 705) (Cell Signaling, Danvers, MA) was performed on adipose tissue and liver sections, respectively, using the ABC kit (Vector Laboratories) according to the manufacturer′s recommendations. As a negative control, staining was performed on selected sections with isotype control. Samples were analyzed with standard light microscopy and a Zeiss AxioImager Z1 microscope system with a charge-coupled device camera and a TissueFAXS automated acquisition system (TissueGnostics, Vienna, Austria), respectively. The percentage of pSTAT3-positive cells of 1,000 cells was determined using HistoQuest software (TissueGnostics).

Stromal vascular cells (SVCs) of GWAT were isolated by collagenase digestion and centrifugation to remove adipocytes as described (24). The percentage of macrophages within SVCs was determined using phycoerythrin-conjugated anti-F4/80 mAb (Abd Serotec) and standard flow cytometric procedures.

Determination of liver triglyceride content. Liver triglycerides were determined following lipid extraction as described previously (30) but by using a commercially available enzymatic reagent (A. Menarini Diagnostics).

Cell culture and OPN treatment in HepG2 cells. Human hepatocellular carcinoma (HepG2) cells (ATCC, Manassas, VA) were grown in RPMI-1640 medium (Invitrogen, Carlsbad, CA) supplemented with 10% (vol/vol) FCS, penicillin/streptomycin (100 units/ml and 100 μg/ml) (Invitrogen) and 2 mmol/l glutamine at 37°C in humidified atmosphere containing 5% CO_2. For stimulation with OPN, cells were plated in six-well plates and grown to confluence before overnight treatment in serum-free RPMI + 1% BSA. Cells were stimulated or not with 0.5 μg/ml recombinant human OPN (Sigma, St. Louis, MO) for 30 min or 2 days, as indicated. Cells were washed twice with ice-cold PBS and lysed in ice-cold lysis buffer containing 1% Triton X-100 (Pierce, Rockford, IL), phosphatase, and protease inhibitors in Tris-buffered saline (pH 7.4) and were subsequently incubated for 30 min on ice. Lysates were cleared from nuclei and cell debris by centrifugation at 13,000 rpm for 1 min and were then prepared for immunoblotting.

Immunoblotting. Identical amounts of protein were separated by SDS-PAGE and blotted onto nitrocellulose membranes (Hybond ECL; Little Chalfont, Amersham, U.K.). Phosphorylated STAT3 (Tyr-705) and total STAT3 were analyzed using respective mouse polyclonal antibodies (Cell Signaling) followed by a horseradish peroxidase–labeled secondary antibody (Accurate, Westbury, NY). Chemiluminescence was generated by a BM chemiluminescence substrate (Roche) and quantified on a Lumi-Imager (Roche).

Phosphorylation of c-Jun NH_2-terminal kinase (JNK) was determined essentially as described (29). Briefly, GWAT was homogenized and lysed on ice for 30 min in Tris-buffered saline, pH 7.4, containing 1% Triton X-100 (Pierce) and phosphatase and protease inhibitors. The tissue extract was cleared from fat, nuclei, and debris by centrifugation. Phosphorylated JNK (Thr-183, Tyr-185) and total JNK were analyzed as described for STAT3 immunblotting using respective rabbit polyclonal antibodies (Cell Signaling).

Reverse transcription and gene expression. Parts of GWAT and liver were immediately snap frozen in liquid nitrogen for RNA isolation. Adipose tissue and liver was homogenized in TRIzol reagent (Invitrogen), and RNA was isolated according to manufacturer's protocol. One microgram of total RNA was treated with DNase I and reverse transcribed into cDNA using Superscript II and random hexamer primers (all Invitrogen). Gene expression normalized to 18S rRNA and Ubiquitin C, respectively, was analyzed by quantitative real-time RT-PCR on an ABI Prism 7000 cylcer using commercial assays-on-demand kits (all Applied Biosystems, Foster City, CA). Alternatively, the expression of following murine genes were quantified by use of self-designed primer pairs and iTaq SYBR Green Supermix (Bio-Rad Laboratories, Hercules, CA): *Tnf* (5′-CCAGACCCTCACACTCAGATCA-3′) forward, (5′-TGGTAT GAGATAGCAAATCGGCT-3′) reverse; *Ccl2* (5′-AGGTCCCTGTCATGCT TCTGG-3′) forward, (5′-CTGCTGCTGGTGATCCTCTTG-3′) reverse; *Tgfb1* (5′-CTACCATGCCAACTTCTGTCTG-3′) forward, (5′-CGGGTTGTGTTGGTT GTAGA-3′) reverse; *Pck1* (5′-AATCACCGCATAGTCTCTGAAGTT-3′) forward, (5′-ACACACACACATGCTCACACAG-3′) reverse; and *G6pc* (5′-CTGGTAGCCCT GTCTTTCTTTG-3′) forward, (5′-TTTCCAGCATTCACACTTTCCT-3′) reverse.

Statistics. All data are given as means ± SE. Comparisons were assessed by unpaired two-tail Student's t test. A P value of ≤0.05 was considered statistically significant.

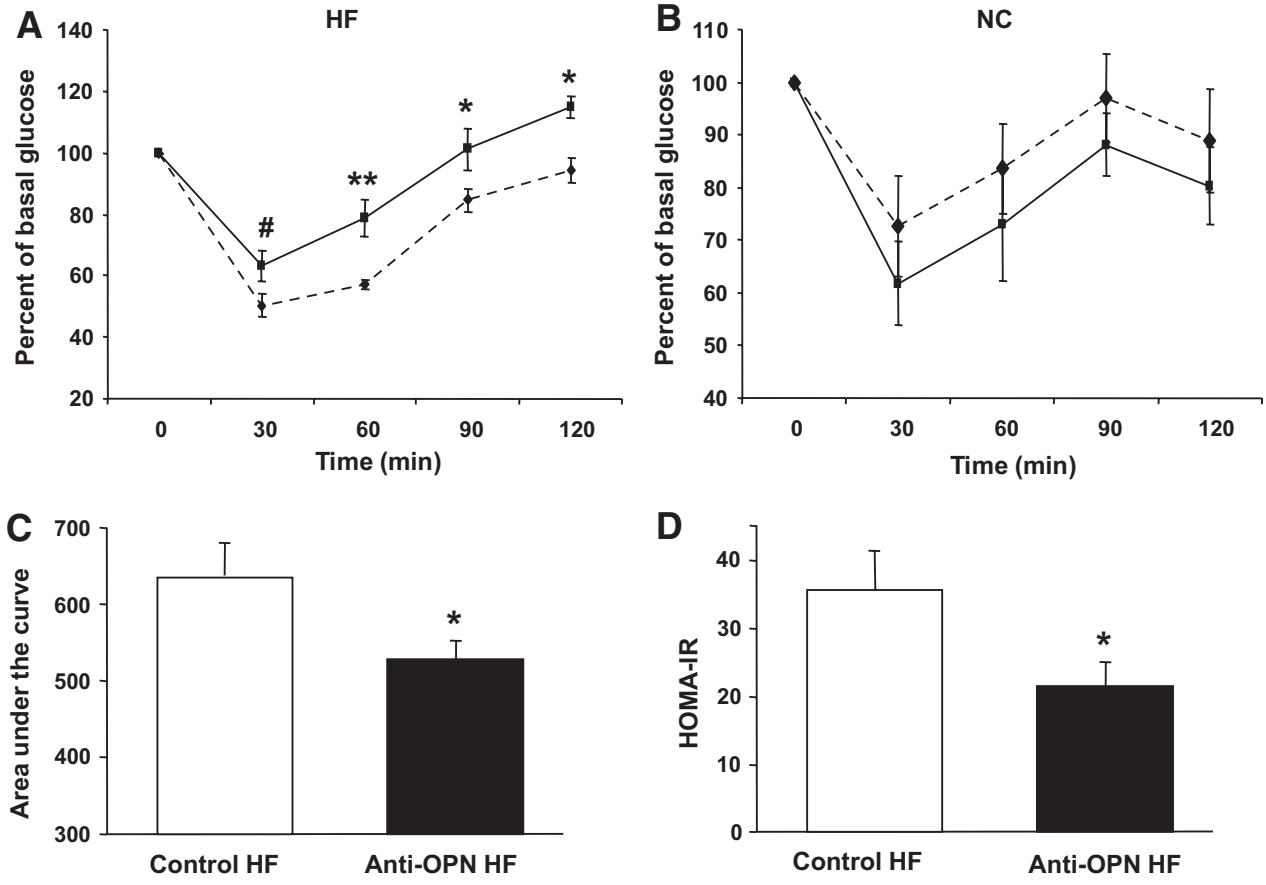

FIG. 1. Insulin sensitivity is improved by OPN neutralization. Mice were fed a high-fat diet (HF) to induce obesity or normal chow (NC), respectively, for 24 weeks and were treated intravenously with an OPN-neutralizing (Anti-OPN) or control antibody three times during 5 days at the end of the feeding period. An ITT was performed in lean and obese OPN antibody-treated (dashed lines) and control antibody–treated (solid lines) mice 1 day after the last antibody application ($n = 5$ per group for NC and $n = 8$ per group for HF). *A* and *B*: Percent of basal glucose during ITT in mice on high-fat diet (*A*) and normal chow (*B*). *C*: Area under the curve. *D*: HOMA-IR was calculated. *$P \leq 0.05$; **$P \leq 0.01$; #$P = 0.06$.

RESULTS

Diet-induced insulin resistance is reversed by antibody-mediated OPN neutralization. We first investigated whether insulin resistance in obese mice is ameliorated by systemic neutralization of OPN action. Male C57BL/6J mice were fed a high-fat diet (HF) or normal chow diet (NC) for 24 weeks to induce obesity and insulin resistance or to serve as lean controls, respectively. Mice from each group were then intravenously treated with a neutralizing anti-mouse OPN antibody or control IgG three times during 5 days. Specificity of the antibody was tested by Western blot detecting OPN protein only in plasma of wild-type but not of OPN-deficient (*Spp1*$^{-/-}$ knockout) mice (supplemental Fig. 1*A* [available in the online appendix at http://diabetes.diabetesjournals.org/cgi/content/full/db09-0404/DC1]).

Animals in the anti-OPN and control groups were of comparable body weight before and after treatment (supplemental Table 1). However, mice of each group weighed slightly, but nonsignificantly, less at the end of the treatment period presumably because they were repeatedly fasted for the insulin and glucose tolerance test. Liver and omental fat pad weight did not differ between antibody-treated and control mice on the respective diet, and anti-OPN treatment did not affect food intake (supplemental Table 1).

Strikingly, treatment with OPN-neutralizing antibody markedly improved insulin sensitivity in obese mice, as shown by significantly reduced blood glucose concentrations at 60, 90, and 120 min of an insulin tolerance test (Fig. 1*A*) and a declined area under the curve (Fig. 1*C*). In addition, insulin resistance as estimated by HOMA-IR was significantly lower after anti-OPN treatment (Fig. 1*D*). Insulin sensitivity was unaltered in NC mice irrespective of anti-OPN treatment (Fig. 1*B*). However, glucose tolerance did not differ between antibody-treated and control mice on either diet (supplemental Fig. 2). Taken together, these data strongly indicate enhanced insulin sensitivity in obese mice upon OPN neutralization. Plasma concentrations of glucose, cholesterol, triglycerides, free fatty acids, adiponectin, leptin, TNF-α, and IL-6 did not significantly differ between groups (supplemental Table 2).

OPN neutralization inhibits macrophage accumulation in obese adipose tissue. To investigate potential mechanisms underlying improved insulin sensitivity following OPN neutralization, we went on to examine adipose tissue inflammation and macrophage accumulation. mRNA expression of *Emr1*, the gene encoding the macrophage marker F4/80, was strikingly increased in obese GWAT (Fig. 2*A*). However, *Emr1* expression was significantly downregulated upon OPN neutralization compared with control antibody treatment in HF mice, while *Emr1* expression was unaffected between NC groups (Fig. 2*A*). In addition, the percentage of F4/80^{+} cells in the SVC

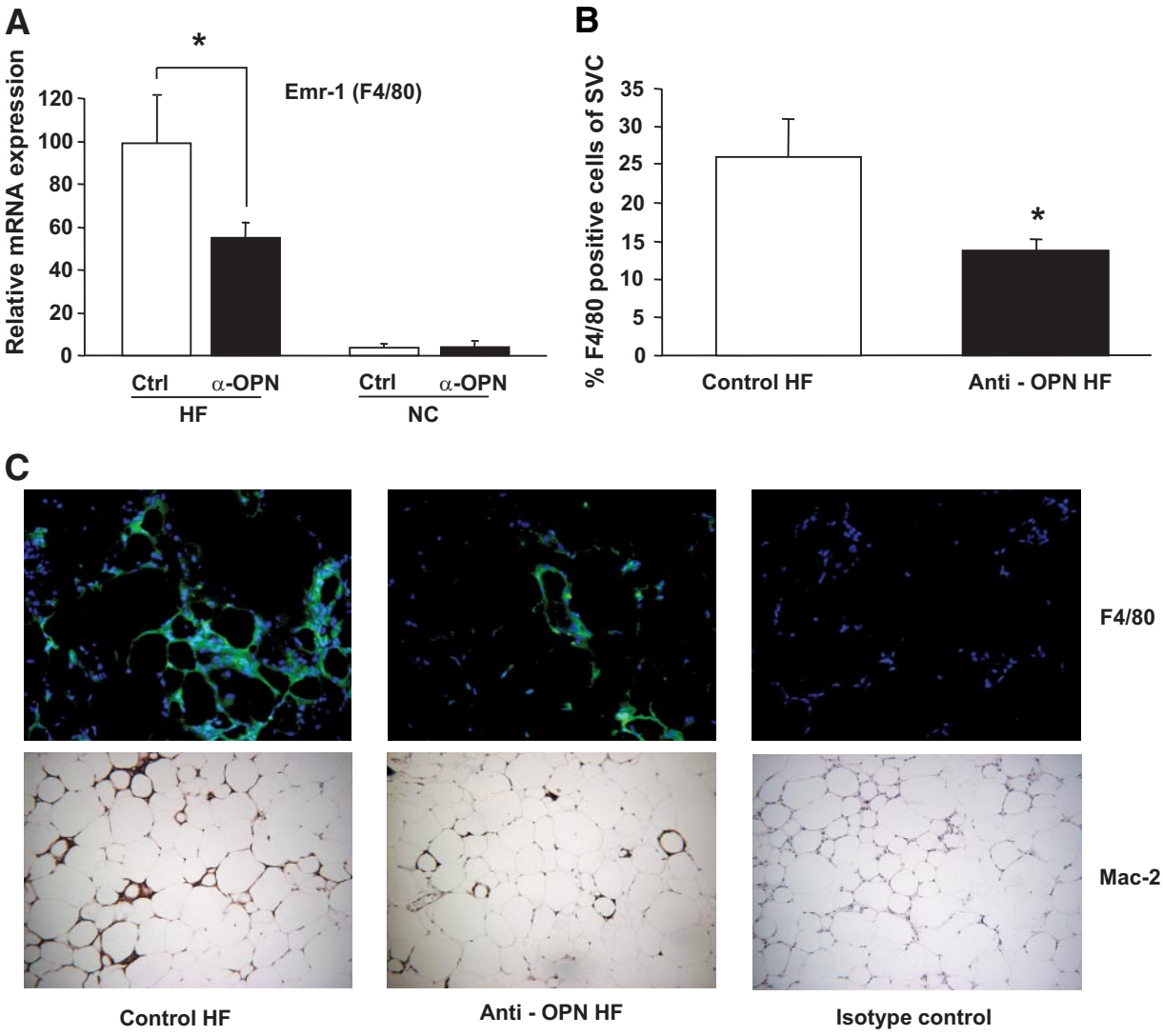

FIG. 2. Adipose tissue macrophage accumulation is reduced by OPN neutralization. Obese high-fat diet–fed (HF) and lean normal chow–fed (NC) mice were treated with OPN-neutralizing (Anti-OPN) or control antibody (n = 8 per group for HF and n = 5 per group for NC mice). *A*: mRNA expression of the macrophage marker F4/80 (encoded by *Emr1* gene) was analyzed in GWAT by real-time RT-PCR. The mean of control HF was set to 100%. *B*: Percentage of macrophages (F4/80-positive cells) in the SVC fraction of GWAT as determined by flow cytometry. *C*: Adipose tissue macrophage accumulation was determined by immunofluorescence of F4/80$^+$ cells (upper row) and immunohistochemical staining of Mac-2$^+$ cells (bottom row) in GWAT isolated from high-fat diet–fed mice after anti-OPN or control antibody treatment. Representative pictures are given in 40-fold magnification. *D*: Adipose tissue macrophages as detected by F4/80 positivity in tissue sections were counted as F4/80$^+$ cells relative to total number of cells. (A high-quality digital representation of this figure is available in the online issue.)

fraction was markedly reduced as determined by fluorescence-activated cell sorting analysis (Fig. 2*B*). Accordingly, the number of macrophages in GWAT, as determined by immunofluorescence (F4/80$^+$) and immunohistochemistry (Mac-2), was significantly lower in obese antibody-treated compared with the HF control mice (Fig. 2*C* and *D*; supplemental Fig. 3*A* and *B*) but did not differ between lean mice (not shown).

Given the rapid reduction of adipose tissue macrophage numbers after OPN neutralization and a potential anti-apoptotic role of OPN in macrophages (31), we hypothesized that enhanced apoptosis in anti-OPN–treated mice could contribute to the disappearance of adipose tissue macrophages. Terminal deoxynucleotidyl transferase–mediated dUTP-biotin nick-end labeling (TUNEL) staining of GWAT sections revealed that the proportion of apoptotic F4/80$^+$ cells was significantly increased by 2.16 ± 0.30-fold in obese OPN antibody-treated compared with control-treated mice (Fig. 3). The abundance of apoptotic nonmacrophages was generally low (<15% of apoptotic cells) and did not differ between the antibody-treated and the control group on a high-fat diet (data not shown). Identical results as for F4/80 staining were obtained for Mac-2 and TUNEL double staining of GWAT sections (supplemental Fig. 3).

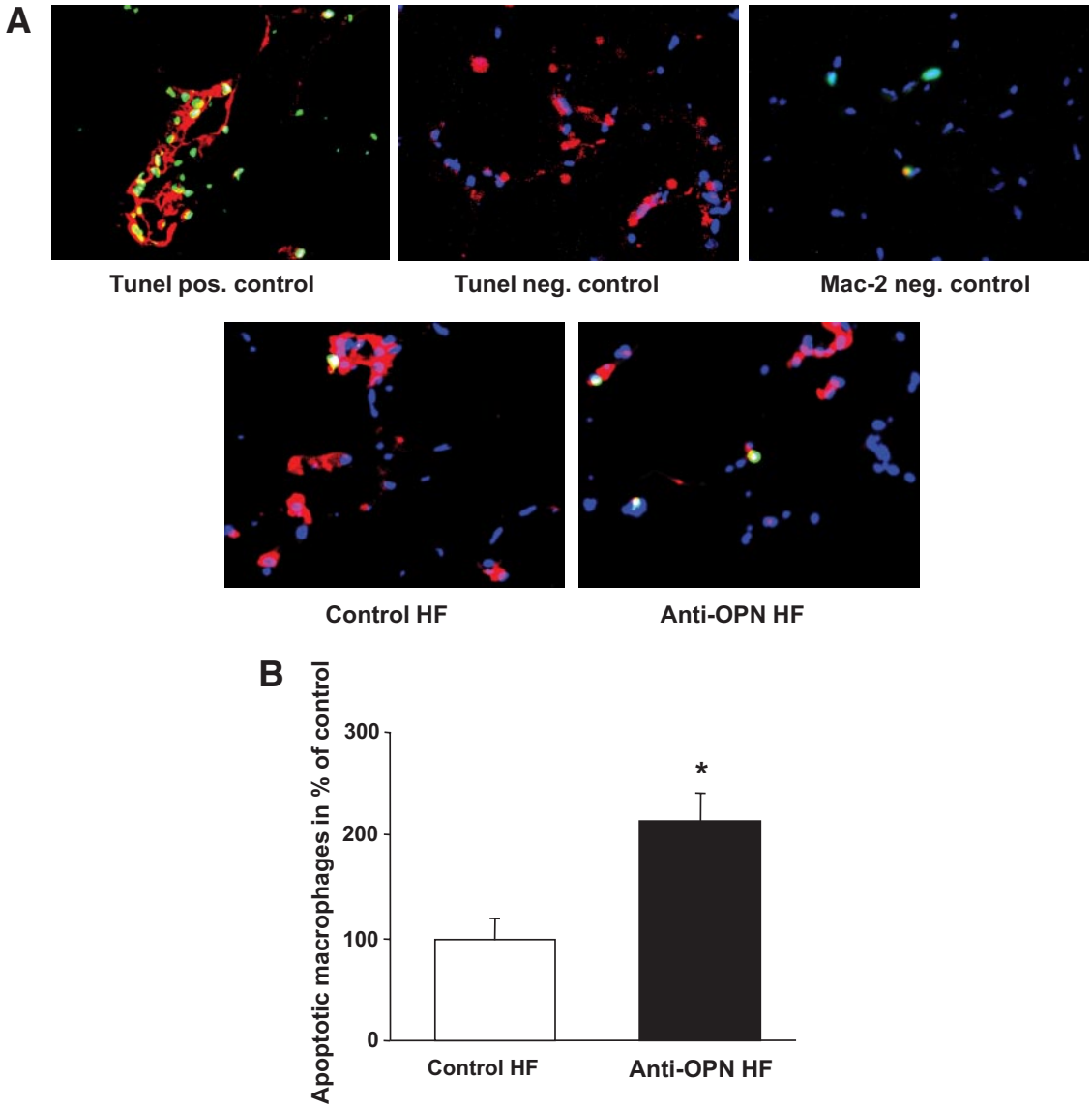

FIG. 3. *A*: **Apoptotic cells were determined by tunel staining (green), macrophages were stained red by immunoflourescence using anti-F4/80 monoclonal antibody on frozen sections. Representative pictures are given.** *B*: **Quantification of apoptotic macrophages (TUNEL and F4/80 double-positive cells per F4/80-positive cells). The mean of Control HF was set to 100%. *$P \leq 0.05$. (A high-quality digital representation of this figure is available in the online issue.)**

Hence, OPN neutralization in obese mice reduces adipose tissue macrophage numbers at least in part by promoting adipose tissue macrophage apoptosis.

OPN neutralization attenuates obesity-induced adipose tissue inflammation. Immunoblot quantification of OPN protein revealed decreased OPN content in obese GWAT after OPN neutralization, even though not statistically significant. (supplemental Fig. 1*B* and *C*). However, OPN plasma concentrations were similar in antibody-treated and control mice and did not differ between lean and obese mice 2 days after the last antibody application (supplemental Table 2). To investigate potential effects of OPN neutralization on inflammatory signaling related to impaired insulin sensitivity in obese mice, we analyzed activation of JNK by determining phosphorylation of JNK1 and JNK2 in GWAT (32). Notably, anti-OPN treatment abolished JNK phosphorylation in obese (Fig. 4*A* and *B*) but not in lean (Fig. 4*C* and *D*) mice. To further determine effects of OPN neutralization on adipose tissue inflammation, we analyzed gene expression of the adipokines IL-6, TNF-α, MCP-1, and IL-10 in GWAT. Notably, IL-6 gene expression in obese mice was markedly decreased upon anti-OPN treatment, while TNF-α, MCP-1, and IL-10 were not significantly reduced (Fig. 4*E* and *F* and supplemental Fig. 4*A* and *B*). GLUT4 and insulin receptor substrate-1, markers of insulin sensitivity, showed a nonsignificant trend to upregulation in adipose tissue of anti-OPN–treated obese mice (supplemental Fig. 4*C* and *D*). However, adiponectin mRNA expression was similar in all groups irrespective of diet and antibody treatment (supplemental Fig. 4*E*). Taken together, these data strongly suggest that OPN neutralization effectively decreases deleterious inflammatory alterations in adipose tissue of obese mice.

Obesity-induced hepatic inflammation is decreased upon OPN neutralization. Anti-OPN treatment nonsignificantly decreased OPN content in liver of obese mice similar to adipose tissue (supplemental Fig. 1*D* and *E*). Given the attenuation of adipose tissue inflammation in antibody-treated HF mice, we investigated whether OPN

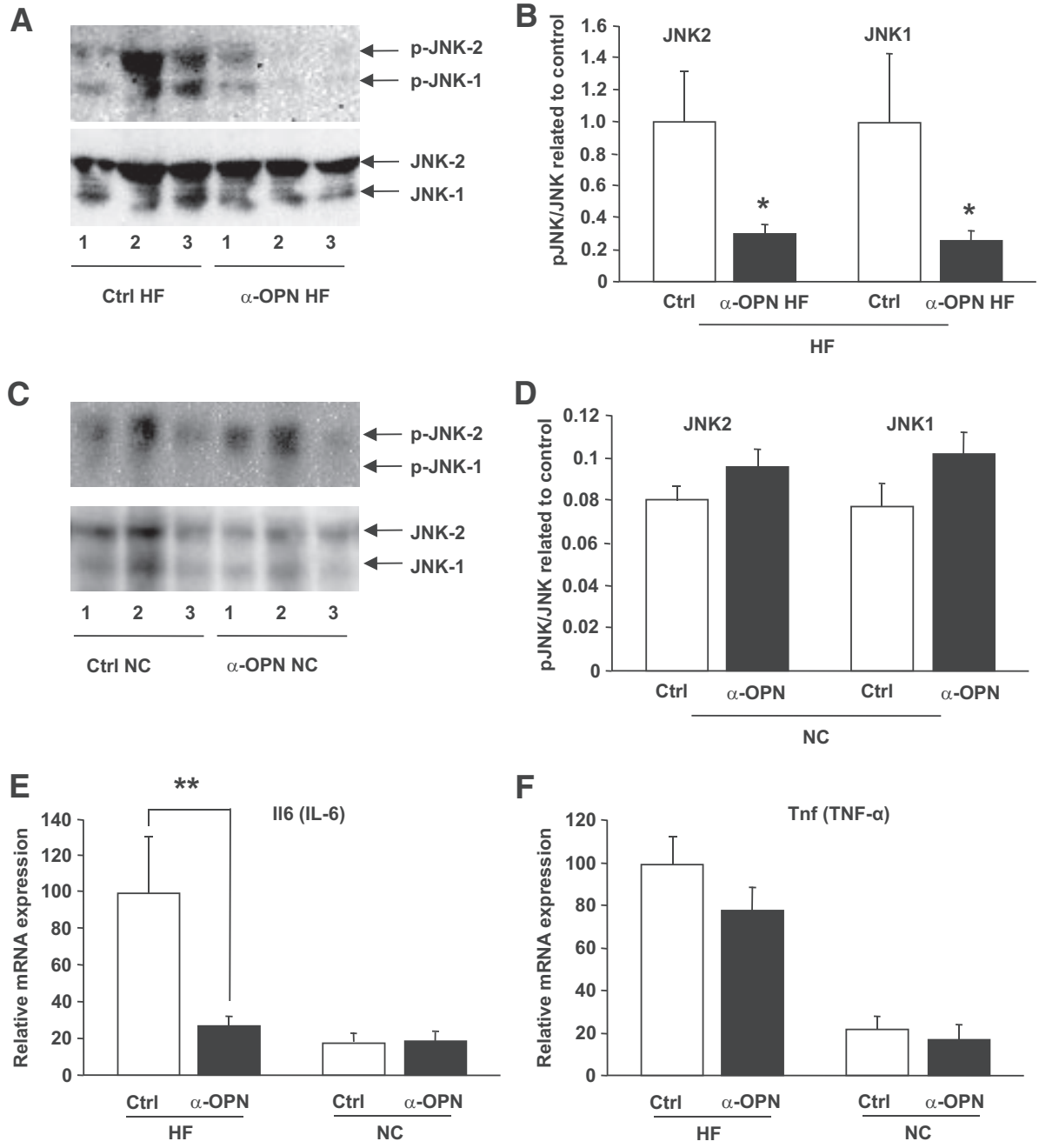

FIG. 4. Adipose tissue inflammatory signaling and cytokine expression is attenuated by OPN neutralization in obese mice. Obese high-fat diet–fed (HF) and lean normal chow–fed (NC) mice were treated with OPN-neutralizing (α-OPN) or control antibody ($n = 8$ per group for HF and $n = 5$ per group for NC mice). *A–D*: Immunoblot analysis and quantification of JNK1 and JNK2 phosphorylation in GWAT. Representative blots are given for obese (*A*) and lean (*C*) adipose tissue. The diagrams show means of the chemiluminescence intensity ratios from phosphorylated versus total JNK protein for obese (*B*) and lean (*D*) anti-OPN– and control-treated mice. *E* and *F*: mRNA expression of the inflammatory genes for IL-6 (*Il6*) (*E*) and TNF-α (*Tnf*) (*F*) was analyzed in GWAT. The mean of Control HF was set to 100%. *$P \leq 0.05$; **$P \leq 0.01$.

neutralization also affects obesity-induced systemic and hepatic inflammation. Systemic concentrations of serum amyloid P (SAP) were markedly elevated in obese control mice but returned to lean levels upon OPN neutralization (86.0 ± 24.4 ng/ml vs. 30.9 ± 8.1 ng/ml; lean control 36.5 ± 6.4 ng/ml; $P < 0.05$; Supplemental Table 2). Plasma concentrations of leptin, IL-6, and TNF-α remained unaffected by OPN treatment in obese mice (supplemental Table 2). Notably, hepatic expression of the inflammatory proteins TNF-α and transforming growth factor (TGF)-β1 was decreased in anti-OPN–treated animals compared with controls (Fig. 5*A* and *B*), whereas expression of the anti-inflammatory IL-10 was significantly enhanced in livers of OPN antibody-treated mice (Fig. 5*C*). Hepatic gene expression of the macrophage marker F4/80 (*Emr1*) was markedly downregulated upon OPN neutralization in obese mice (Fig. 5*D*). Accordingly, hepatic macrophage accumulation as determined by immunoflourescence (Fig. 5*E* and *F*) and immunohistochemistry (supplemental Fig. 5*A*) was attenuated upon anti-OPN treatment. TUNEL staining revealed that, similar to adipose tissue, the proportion of apoptotic macrophages was significantly increased in obese anti-OPN– compared with control-treated animals (Fig. 5*E* and *G*).

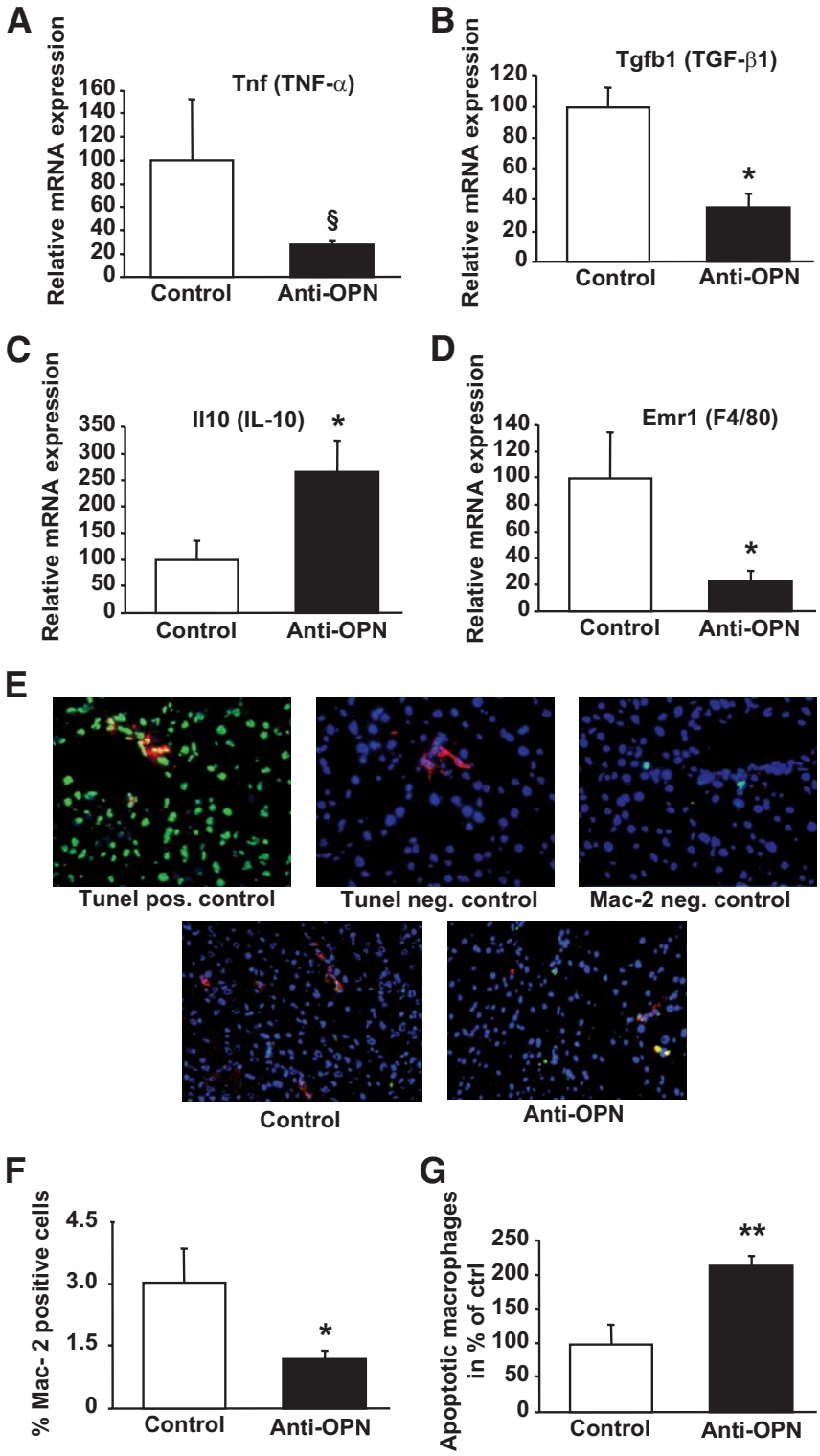

FIG. 5. OPN neutralization decreases hepatic inflammation. Obese high-fat diet–fed (HF) mice were treated with OPN-neutralizing (Anti-OPN) or control (n = 8 per group) antibody. Hepatic expression of genes for the inflammatory cytokines TNF-α (*Tnf*) (*A*) and TGF-β1 (*Tgfb1*) (*B*), the anti-inflammatory IL-10 (*Il10*) (*C*), and for the macrophage marker F4/80 (*Emr1*) (*D*) was analyzed by real-time RT-PCR. The mean of Control was set to 100%. *E–G*: Hepatic macrophage accumulation and apoptosis. *E*: Macrophages were stained red by immunoflourescence using Mac-2 monoclonal antibody on frozen sections of livers isolated from high-fat diet–fed mice after anti-OPN or control treatment. Apoptotic cells were determined by TUNEL staining (green). Representative pictures are given in 40-fold magnification. *F*: Hepatic macrophages were counted as Mac-2$^+$ cells relative to total number of cells. *G*: Quantification of apoptotic macrophages (TUNEL and Mac-2 double-positive cells per Mac-2–positive cells). The mean of Control was set to 100%. *$P \leq 0.05$; **$P \leq 0.01$. (A high-quality color representation of this figure is available in the online issue.)

Inflammatory alterations in liver could be related to lipid accumulation. However, liver triglyceride content was similar in the anti-OPN and control group kept on a high-fat diet (supplemental Fig. 5*B*). Moreover, no change in lipid droplet size by short-term OPN neutralization was evident in hematoxylin and eosin–stained liver sections

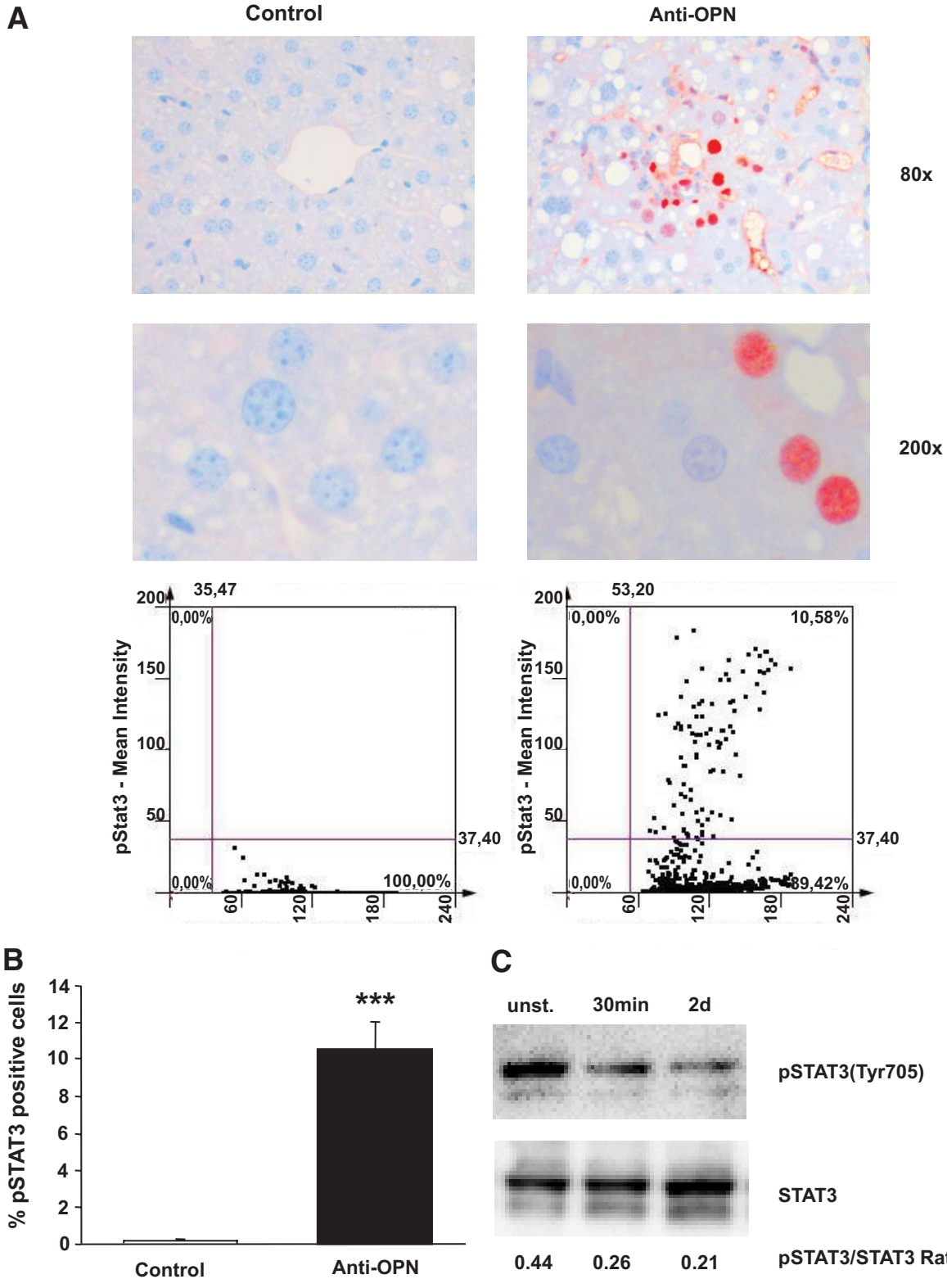

FIG. 6. OPN interferes with hepatic STAT3 activation in obesity. *A–C*: Obese high-fat diet–fed (HF) mice were treated with OPN-neutralizing (Anti-OPN) or control (n = 8 per group) antibody. STAT phosphorylation was determined by immunhistochemical analysis of pSTAT(Tyr705) on paraffin sections of livers isolated from high-fat diet–fed mice after anti-OPN or control treatment. *A*: Representative immunohistochemical pictures are given in 80- and 200-fold magnification, respectively. The representative TissueFaxs scattergramm shows the percentage of pSTAT(Tyr705) positive cells in liver; (n = 5 per group). *B*: Quantification of pSTAT3-positive cells determined by TissueFaxs. *C*: Immunoblot analysis of STAT3 tyrosine 705 phosphorylation in HepG2 cells. Cells were stimulated or not with 0.5 μg/ml human recombinant OPN for 30 min and 2 days followed by immunoblotting for pSTAT3(Tyr705) and STAT3. A representative blot is given along with mean ratios. ***$P \leq 0.001$. (A high-quality digital representation of this figure is available in the online issue.)

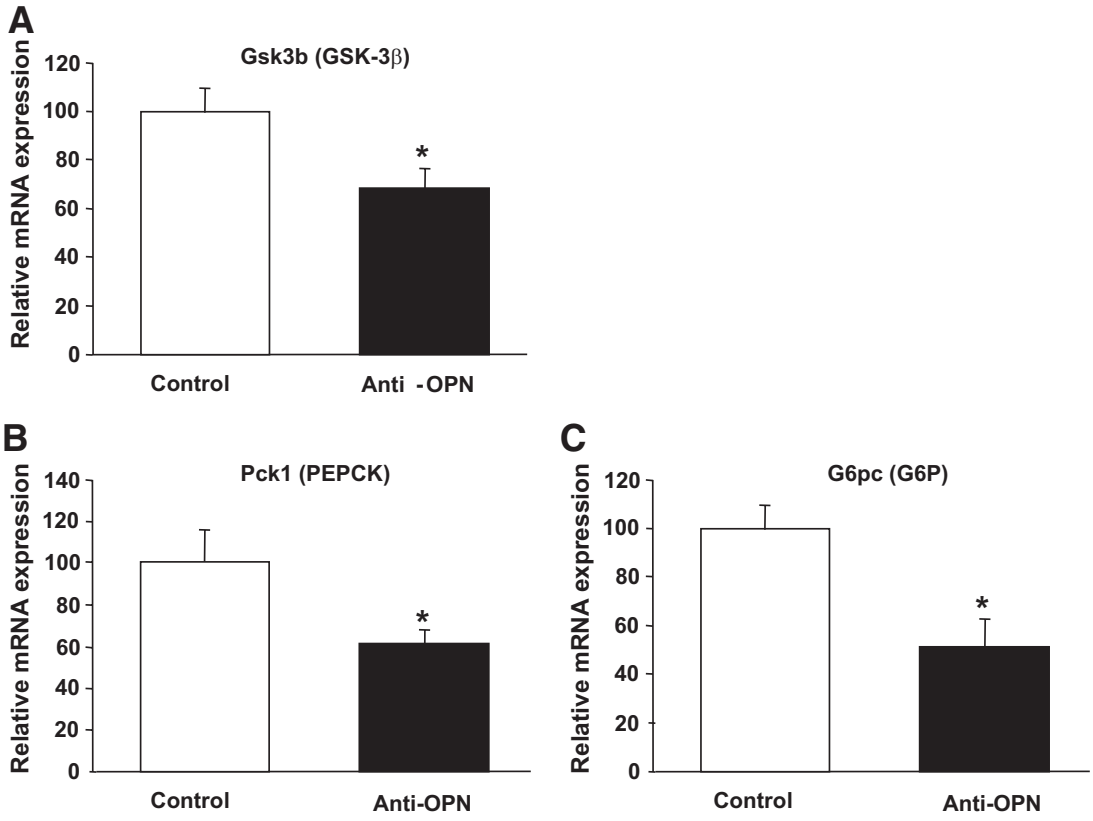

FIG. 7. OPN neutralization downregulates expression of hepatic gluconeogenic markers. Obese high-fat diet–fed (HF) mice were treated with OPN-neutralizing or control antibody ($n = 8$ per group). Hepatic mRNA expression of genes encoding GSK-3β (*Gsk3b*) (*A*) and the gluconeogenic enzymes PEPCK (*Pck1*) (*B*) and G6P (*G6pc*) (*C*) was analyzed. *$P \leq 0.05$.

(supplemental Fig. 5*C*). Gene expression of the lipogenic markers fatty acid synthase (FAS) and sterol regulatory element–binding protein-1c (SREBP-1c) did neither show any difference by anti-OPN treatment in obese mice (supplemental Fig. 5*D* and *E*). Plasma concentrations of the hepatic enzymes ALT and AST were unaffected by anti-OPN treatment in obese mice (supplemental Fig. 5*F* and *G*). These results indicate that short-term neutralization of OPN attenuates hepatic inflammation and macrophage accumulation in obese mice independent of hepatic steatosis.

Antibody-mediated OPN neutralization rescues hepatic STAT3 activation. Hepatic STAT3 signaling is essential for normal glucose homeostasis (33,34), and IL-10 is known to induce hepatic STAT3 phosphorylation (35,36). To investigate whether OPN neutralization affects hepatic STAT3 activation in obesity, we studied STAT3 activation in livers of anti-OPN– and control antibody–treated obese mice. Hepatic STAT3 tyrosine phosphorylation was markedly increased in obese anti-OPN– compared with control-treated mice, as shown by immunohistochemistry (Fig. 6*A* and *B*). To investigate whether OPN directly affects STAT3 activation, we treated human hepatocellular carcinoma (HepG2) cells with or without OPN and quantified STAT3 tyrosine phosphorylation by immunoblot. Indeed, OPN treatment markedly decreased basal pSTAT3 in HepG2 cells (Fig. 6*C*), indicating a direct inhibitory effect of OPN on STAT3 tyrosine phosphorylation.

OPN neutralization downregulates expression of hepatic gluconeogenic markers. Since STAT3 sensitizes insulin signaling by negatively regulating glycogen synthase kinase-3β (GSK-3β; gene *Gsk3b*) expression, we studied mRNA expression of GSK-3β in liver of anti-OPN–treated and control mice. We observed a significant decrease in hepatic GSK-3β gene expression upon OPN neutralization (Fig. 7*A*). Insulin signaling in the liver leads to suppression of gluconeogenesis. The key gluconeogenic enzymes phosphoenolpyruvate carboxykinase (PEPCK; gene *Pck1*) and glucose 6 phosphatase (G6P; gene *G6pc*) that are targets of GSK-3β (37) and relevant markers of hepatic insulin resistance (38), were both significantly downregulated upon anti-OPN treatment (Fig. 7*B* and *C*). Taken together, these data indicate that OPN promotes hepatic gluconeogenesis, thereby contributing to obesity-induced insulin resistance.

DISCUSSION

The increasing prevalence of obesity demands novel preventive and therapeutic approaches to treat obesity-associated complications, particularly insulin resistance, that leads to type 2 diabetes and promotes cardiovascular disease. We and others have recently reported that OPN expression is considerably upregulated in human obesity as well as mouse models of genetic and diet-induced obesity (24–26). Here, we show that antibody-mediated neutralization of OPN attenuates adipose tissue, hepatic, and systemic inflammation and markedly improves insulin sensitivity in murine obesity.

A recent publication demonstrated that genetic OPN deficiency attenuates adipose tissue inflammation and insulin resistance in a model of murine diet-induced obesity (26). This genetic approach shows that obesity-induced metabolic alterations are improved if OPN is

already absent during development, including enlargement of fat depots. Here, we show that short-term OPN neutralization attenuates inflammation and insulin resistance when obesity has already been established. In addition, our results indicate that negative OPN effects on glucose metabolism are obesity dependent because OPN neutralization did not alter insulin sensitivity and adipose tissue inflammation in lean mice (Figs. 1–4). Other than in genetic OPN deficiency (26), glucose tolerance was apparently not affected by short-term OPN neutralization. However, it remains elusive whether a long-term treatment with an OPN neutralizing antibody is able to restore β-cell function and therefore improve glucose tolerance in obesity. Insulin resistance is rapidly reversible, particularly in mice (39). Similar to our data on OPN neutralization, treatment with an anti–TNF-α monoclonal antibody rapidly improved insulin sensitivity in patients with rheumatoid arthritis (40). These and our findings reveal a potential therapeutic impact of targeting obesity-associated inflammatory mediators linked to insulin resistance and the metabolic syndrome.

Obesity-driven insulin resistance is associated with macrophage accumulation in adipose tissue (6). OPN is involved in macrophage migration and macrophage-driven inflammatory disorders (11,15,16). Treatment with anti-OPN antibody for only 5 days significantly decreased adipose tissue and liver macrophage numbers in obese mice (Fig. 2 and Fig. 5*D–F*). Similarly, blocking of the chemokine receptor CCR2 for 9 days resulted in a significant reduction of adipose tissue macrophage accumulation (5). Thus, macrophage turnover appears to be rather high in obese murine adipose tissue.

OPN has previously been shown to be a survival factor for macrophages in HIV-induced brain disease (31) and for T-cells in an arthritis model (41). Here, we show that the rapid reduction of adipose tissue and liver macrophages by OPN neutralization was accompanied by a significantly increased number of apoptotic macrophages (Fig. 3 and Fig. 5*E* and *G*; Supplemental Fig. 3), indicating that macrophage apoptosis contributes to reduced macrophage abundance in anti-OPN–treated mice. Aside from enhanced macrophage apoptosis, disturbed cell migration could contribute to the reduction of macrophages in adipose tissue and liver of anti-OPN–treated mice, since OPN is well-known to be critically involved in migration of monocytes and macrophages (11,26). Hence, the marked obesity-induced upregulation of OPN expression in adipose tissue and liver (24) could promote macrophage accumulation in both tissues not only by stimulating cell migration (42) but also by preventing macrophage apoptosis.

Since we did not observe reduced OPN plasma concentrations after anti-OPN treatment (supplemental Table 2), we assume functional neutralization of OPN to underlie the decrease in adipose tissue and liver macrophage numbers (43,44). Since macrophages are the major source of OPN at least in adipose tissue (24), the somewhat reduced tissue OPN content following OPN neutralization is probably due to diminished local production.

A high-fat diet causes activation of the JNK pathway that leads to insulin resistance by serine phosphorylation of insulin receptor substrate proteins (4,32,45). OPN neutralization inhibited inflammatory signaling by negatively regulating JNK1 and JNK2 phosphorylation in obese adipose tissue (Fig. 4*A* and *B*). In contrast to reduced GWAT expression of IL-6, a potent mediator between obesity-induced adipose tissue inflammation and insulin resistance (46), TNF-α, MCP-1, and IL-10 expression remained unaffected (Fig. 4*E* and *F* and supplemental Fig. 4*A* and *B*). Our data are in accordance with a recent publication showing that adipose tissue–specific deletion of JNK1 significantly reduced obesity-induced insulin resistance and IL-6 expression in adipose tissue, while TNF-α remained unaltered (47). Taken together, these results emphasize abolished JNK activation to be a crucial mechanism for anti-inflammatory effects of OPN neutralization in adipose tissue.

Obesity is a prominent risk factor for the development of nonalcoholic fatty liver disease including steatohepatitis (NAFLD/NASH), which is related to hepatic insulin resistance (48,49). Macrophages are the primary source of hepatic inflammatory cytokines such as TNF-α, which critically contributes to hepatic insulin resistance and hepatic steatosis in diet-induced obesity (50). Treatment with anti-OPN decreased hepatic expression of the macrophage marker F4/80 and of inflammatory cytokines TNF-α and TGF-β (Fig. 5*A*, *B*, and *D*). Recently, IL-10 was demonstrated to act as a protective factor against diet-induced insulin resistance and inflammation in liver (51). Here, we show that in contrast to adipose tissue, hepatic IL-10 expression was significantly elevated upon anti-OPN treatment (Fig. 5*C*). This tissue-specific difference in cytokine response to OPN neutralization might be attributed to the fact that in liver not only macrophages but also hepatocytes produce IL-10 (52). Taken together, OPN neutralization attenuated hepatic inflammation in obesity, which is in accordance with a reported role of OPN in the pathogenesis of NASH elicited by methionine and choline diet (22,23).

Elevated expression of the gluconeogenic enzymes PEPCK and G6P is a hallmark of hepatic insulin resistance (38). STAT3 is a critical transcription factor for sensitizing insulin signaling in hepatocytes through suppression of GSK-3β, PEPCK, and G6P (33,37,53). Whereas OPN neutralization increased hepatic STAT3 activation in vivo, OPN stimulation diminished STAT3 phosphorylation in HepG2 cells in vitro (Fig. 6). Hence, we provide a novel link between OPN and STAT3 activation, indicating that beneficial effects of OPN neutralization on hepatic gluconeogenesis could be mediated by STAT3. Effects of short-term OPN neutralization on hepatic inflammation and gluconeogenic enzyme expression cannot be attributed to reduced hepatic steatosis, as shown by unaltered hepatic triglyceride content, liver histology, and gene expression of lipogenic markers (supplemental Fig. 5*B–E*). These data suggest that STAT3 activation following short-term anti-OPN treatment specifically regulates gluconeogenesis without affecting lipogenesis. However, it remains elusive whether long-term treatment with an OPN neutralizing antibody is able to prevent or reverse hepatic steatosis and NAFLD.

Circulating concentrations of adiponectin and leptin, adipokines known to impact liver function (54), were not affected by OPN neutralization (supplemental Table 2). However, the plasma concentration of the classical murine inflammatory marker SAP that is produced by hepatocytes (55) was normalized by anti-OPN treatment (supplemental Table 2), corroborating attenuation of hepatic inflammation. Whether systemic or local hepatic effects of OPN neutralization underlie the reduction of the inflammatory marker SAP remains elusive. Nevertheless, these data indicate that OPN neutralization reduces hepatic inflam-

mation and improve hepatic regulation of glucose homeostasis in obesity.

Our studies revealed a dual role of OPN in obesity-associated insulin resistance by showing that at least two organs could contribute to improved insulin sensitivity upon OPN neutralization. On the one hand, OPN neutralization interferes with diet-induced macrophage accumulation and inflammatory signaling in adipose tissue, well known to be associated with insulin resistance. On the other hand, we demonstrate that OPN critically affects macrophage infiltration, STAT3 signaling, and regulation of gluconeogenesis in liver. In conclusion, neutralization of OPN significantly attenuates obesity-induced inflammation and insulin resistance, implicating that targeting OPN action could improve metabolic regulation and cardiovascular risk in obese patients.

ACKNOWLEDGMENTS

This work was supported by the Austrian Science Fund (project no. P18776-B11 and as part of the CCHD doctoral program W1205-B09) and the European Community's 7th Framework Programme (FP7/2007-2013) under grant agreement no. 201608 (all to T.M.S.).

No potential conflicts of interest relevant to this article were reported.

We thank Helga Schachner, Liliana-Imi Ionasz, Monika Sulzer, and Ing. Peter Nowotny for excellent technical assistance.

REFERENCES

1. Despres JP, Lemieux I. Abdominal obesity and metabolic syndrome. Nature 2006;444:881–887
2. Bastard JP, Maachi M, Lagathu C, Kim MJ, Caron M, Vidal H, Capeau J, Feve B. Recent advances in the relationship between obesity, inflammation, and insulin resistance. Eur Cytokine Netw 2006;17:4–12
3. Shoelson SE, Herrero L, Naaz A. Obesity, inflammation, and insulin resistance. Gastroenterology 2007;132:2169–2180
4. Hotamisligil GS. Inflammation and metabolic disorders. Nature 2006;444:860–867
5. Weisberg SP, Hunter D, Huber R, Lemieux J, Slaymaker S, Vaddi K, Charo I, Leibel RL, Ferrante AW Jr: CCR2 modulates inflammatory and metabolic effects of high-fat feeding. J Clin Invest 2006;116:115–124
6. Weisberg SP, McCann D, Desai M, Rosenbaum M, Leibel RL, Ferrante AW Jr: Obesity is associated with macrophage accumulation in adipose tissue. J Clin Invest 2003;112:1796–1808
7. Fain JN. Release of interleukins and other inflammatory cytokines by human adipose tissue is enhanced in obesity and primarily due to the nonfat cells. Vitam Horm 2006;74:443–477
8. Curat CA, Wegner V, Sengenes C, Miranville A, Tonus C, Busse R, Bouloumie A. Macrophages in human visceral adipose tissue: increased accumulation in obesity and a source of resistin and visfatin. Diabetologia 2006;49:744–747
9. Zeyda M, Farmer D, Todoric J, Aszmann O, Speiser M, Gyori G, Zlabinger GJ, Stulnig TM. Human adipose tissue macrophages are of an anti-inflammatory phenotype but capable of excessive pro-inflammatory mediator production. Int J Obes (Lond) 2007;31:1420–1428
10. Mazzali M, Kipari T, Ophascharoensuk V, Wesson JA, Johnson R, Hughes J. Osteopontin: a molecule for all seasons. QJM 2002;95:3–13
11. Standal T, Borset M, Sundan A. Role of osteopontin in adhesion, migration, cell survival and bone remodeling. Exp Oncol 2004;26:179–184
12. Rangaswami H, Bulbule A, Kundu GC. Osteopontin: role in cell signaling and cancer progression. Trends Cell Biol 2006;16:79–87
13. Xu G, Nie H, Li N, Zheng W, Zhang D, Feng G, Ni L, Xu R, Hong J, Zhang JZ. Role of osteopontin in amplification and perpetuation of rheumatoid synovitis. J Clin Invest 2005;115:1060–1067
14. Teti A, Farina AR, Villanova I, Tiberio A, Tacconelli A, Sciortino G, Chambers AF, Gulino A, Mackay AR. Activation of MMP-2 by human GCT23 giant cell tumour cells induced by osteopontin, bone sialoprotein and GRGDSP peptides is RGD and cell shape change dependent. Int J Cancer 1998;77:82–93
15. Xu G, Sun W, He D, Wang L, Zheng W, Nie H, Ni L, Zhang D, Li N, Zhang J. Overexpression of osteopontin in rheumatoid synovial mononuclear cells is associated with joint inflammation, not with genetic polymorphism. J Rheumatol 2005;32:410–416
16. Isoda K, Kamezawa Y, Ayaori M, Kusuhara M, Tada N, Ohsuzu F. Osteopontin transgenic mice fed a high-cholesterol diet develop early fatty-streak lesions. Circulation 2003;107:679–681
17. Takemoto M, Yokote K, Nishimura M, Shigematsu T, Hasegawa T, Kon S, Uede T, Matsumoto T, Saito Y, Mori S. Enhanced expression of osteopontin in human diabetic artery and analysis of its functional role in accelerated atherogenesis. Arterioscler Thromb Vasc Biol 2000;20:624–628
18. Ramaiah SK, Rittling S. Pathophysiological role of osteopontin in hepatic inflammation, toxicity, and cancer. Toxicol Sci 2008;103:4–13
19. Bertola A, Deveaux V, Bonnafous S, Rousseau D, Anty R, Wakkach A, Dahman M, Tordjman J, Clément K, McQuaid SE, Frayn KN, Huet PM, Gugenheim J, Lotersztajn S, Le Marchand-Brustel Y, Tran A, Gual P. Elevated expression of osteopontin may be related to adipose tissue macrophage accumulation and liver steatosis in morbid obesity. Diabetes 2009;58:125–133
20. Wang Y, Mochida S, Kawashima R, Inao M, Matsui A, YouLuTu ZY, Nagoshi S, Uede T, Fujiwara K. Increased expression of osteopontin in activated Kupffer cells and hepatic macrophages during macrophage migration in Propionibacterium acnes-treated rat liver. J Gastroenterol 2000;35:696–701
21. Kawashima R, Mochida S, Matsui A, YouLuTuZ Y, Ishikawa K, Toshima K, Yamanobe F, Inao M, Ikeda H, Ohno A, Nagoshi S, Uede T, Fujiwara K. Expression of osteopontin in Kupffer cells and hepatic macrophages and Stellate cells in rat liver after carbon tetrachloride intoxication: a possible factor for macrophage migration into hepatic necrotic areas. Biochem Biophys Res Commun 1999;256:527–531
22. Sahai A, Malladi P, Melin-Aldana H, Green RM, Whitington PF. Upregulation of osteopontin expression is involved in the development of nonalcoholic steatohepatitis in a dietary murine model. Am J Physiol Gastrointest Liver Physiol 2004;287:G264–G273
23. Sahai A, Malladi P, Pan X, Paul R, Melin-Aldana H, Green RM, Whitington PF. Obese and diabetic db/db mice develop marked liver fibrosis in a model of nonalcoholic steatohepatitis: role of short-form leptin receptors and osteopontin. Am J Physiol Gastrointest Liver Physiol 2004;287:G1035–G1043
24. Kiefer FW, Zeyda M, Todoric J, Huber J, Geyeregger R, Weichhart T, Aszmann O, Ludvik B, Silberhumer GR, Prager G, Stulnig TM. Osteopontin expression in human and murine obesity: extensive local up-regulation in adipose tissue but minimal systemic alterations. Endocrinology 2008;149:1350–1357
25. Gómez-Ambrosi J, Catalán V, Ramírez B, Rodríguez A, Colina I, Silva C, Rotellar F, Mugueta C, Gil MJ, Cienfuegos JA, Salvador J, Frühbeck G. Plasma osteopontin levels and expression in adipose tissue are increased in obesity. J Clin Endocrinol Metab 2007;92:3719–3727
26. Nomiyama T, Perez-Tilve D, Ogawa D, Gizard F, Zhao Y, Heywood EB, Jones KL, Kawamori R, Cassis LA, Tschöp MH, Bruemmer D. Osteopontin mediates obesity-induced adipose tissue macrophage infiltration and insulin resistance in mice. J Clin Invest 2007;117:2877–2888
27. Riedl M, Vila G, Maier C, Handisurya A, Shakeri-Manesch S, Prager G, Wagner O, Kautzky-Willer A, Ludvik B, Clodi M, Luger A. Plasma osteopontin increases after bariatric surgery and correlates with markers of bone turnover but not with insulin resistance. J Clin Endocrinol Metab 2008;93:2307–2312
28. Ferrannini E, Mari A. How to measure insulin sensitivity. J Hypertens 1998;16:895–906
29. Todoric J, Loffler M, Huber J, Bilban M, Reimers M, Kadl A, Zeyda M, Waldhausl W, Stulnig TM. Adipose tissue inflammation induced by high-fat diet in obese diabetic mice is prevented by n-3 polyunsaturated fatty acids. Diabetologia 2006;49:2109–2119
30. Haemmerle G, Zimmermann R, Strauss JG, Kratky D, Riederer M, Knipping G, Zechner R. Hormone-sensitive lipase deficiency in mice changes the plasma lipid profile by affecting the tissue-specific expression pattern of lipoprotein lipase in adipose tissue and muscle. J Biol Chem 2002;277:12946–12952
31. Burdo TH, Wood MR, Fox HS. Osteopontin prevents monocyte recirculation and apoptosis. J Leukoc Biol 2007;81:1504–1511
32. Hirosumi J, Tuncman G, Chang L, Gorgun CZ, Uysal KT, Maeda K, Karin M, Hotamisligil GS. A central role for JNK in obesity and insulin resistance. Nature 2002;420:333–336
33. Inoue H, Ogawa W, Ozaki M, Haga S, Matsumoto M, Furukawa K, Hashimoto N, Kido Y, Mori T, Sakaue H, Teshigawara K, Jin S, Iguchi H, Hiramatsu R, LeRoith D, Takeda K, Akira S, Kasuga M. Role of STAT-3 in regulation of hepatic gluconeogenic genes and carbohydrate metabolism in vivo. Nat Med 2004;10:168–174
34. Koch L, Wunderlich FT, Seibler J, Konner AC, Hampel B, Irlenbusch S,

Brabant G, Kahn CR, Schwenk F, Bruning JC. Central insulin action regulates peripheral glucose and fat metabolism in mice. J Clin Invest 2008;118:2132–2147
35. Ji JD, Kim HJ, Rho YH, Choi SJ, Lee YH, Cheon HJ, Sohn J, Song GG. Inhibition of IL-10-induced STAT3 activation by 15-deoxy-delta12,14-prostaglandin J2. Rheumatology (Oxford) 2005;44:983–988
36. Shen X, Hong F, Nguyen VA, Gao B. IL-10 attenuates IFN-alpha-activated STAT1 in the liver: involvement of SOCS2 and SOCS3. FEBS Lett 2000; 480:132–136
37. Lochhead PA, Coghlan M, Rice SQ, Sutherland C. Inhibition of GSK-3 selectively reduces glucose-6-phosphatase and phosphatase and phosphoenolypyruvate carboxykinase gene expression. Diabetes 2001;50:937–946
38. Sun Y, Liu S, Ferguson S, Wang L, Klepcyk P, Yun JS, Friedman JE. Phosphoenolpyruvate carboxykinase overexpression selectively attenuates insulin signaling and hepatic insulin sensitivity in transgenic mice. J Biol Chem 2002;277:23301–23307
39. Jung R. Endocrinological aspects of obesity. Clin Endocrinol Metab 1984;13:597–612
40. Gonzalez-Gay MA, De Matias JM, Gonzalez-Juanatey C, Garcia-Porrua C, Sanchez-Andrade A, Martin J, Llorca J. Anti-tumor necrosis factor-alpha blockade improves insulin resistance in patients with rheumatoid arthritis. Clin Exp Rheumatol 2006;24:83–86
41. Fan K, Dai J, Wang H, Wei H, Cao Z, Hou S, Qian W, Wang H, Li B, Zhao J, Xu H, Yang C, Guo Y. Treatment of collagen-induced arthritis with an anti-osteopontin monoclonal antibody through promotion of apoptosis of both murine and human activated T cells. Arthritis Rheum 2008;58:2041–2052
42. Zhu B, Suzuki K, Goldberg HA, Rittling SR, Denhardt DT, McCulloch CA, Sodek J. Osteopontin modulates CD44-dependent chemotaxis of peritoneal macrophages through G-protein-coupled receptors: evidence of a role for an intracellular form of osteopontin. J Cell Physiol 2004;198:155–167
43. Banerjee A, Apte UM, Smith R, Ramaiah SK. Higher neutrophil infiltration mediated by osteopontin is a likely contributing factor to the increased susceptibility of females to alcoholic liver disease. J Pathol 2006;208:473–485
44. Koguchi Y, Kawakami K, Uezu K, Fukushima K, Kon S, Maeda M, Nakamoto A, Owan I, Kuba M, Kudeken N, Azuma M, Yara S, Shinzato T, Higa F, Tateyama M, Kadota J, Mukae H, Kohno S, Uede T, Saito A. High plasma osteopontin level and its relationship with interleukin-12-mediated type 1 T helper cell response in tuberculosis. Am J Respir Crit Care Med 2003;167:1355–1359
45. Aguirre V, Uchida T, Yenush L, Davis R, White MF. The c-Jun NH(2)-terminal kinase promotes insulin resistance during association with insulin receptor substrate-1 and phosphorylation of Ser(307). J Biol Chem 2000; 275:9047–9054
46. Kern PA, Ranganathan S, Li C, Wood L, Ranganathan G. Adipose tissue tumor necrosis factor and interleukin-6 expression in human obesity and insulin resistance. Am J Physiol Endocrinol Metab 2001;280:E745–E751
47. Sabio G, Das M, Mora A, Zhang Z, Jun JY, Ko HJ, Barrett T, Kim JK, Davis RJ. A stress signaling pathway in adipose tissue regulates hepatic insulin resistance. Science 2008;322:1539–1543
48. Yeh MM, Brunt EM. Pathology of nonalcoholic fatty liver disease. Am J Clin Pathol 2007;128:837–847
49. Diehl AM. Nonalcoholic steatohepatitis. Semin Liver Dis 1999;19:221–229
50. De Taeye BM, Novitskaya T, McGuinness OP, Gleaves L, Medda M, Covington JW, Vaughan DE. Macrophage TNF-alpha contributes to insulin resistance and hepatic steatosis in diet-induced obesity. Am J Physiol Endocrinol Metab 2007;293:E713–E725
51. Cintra DE, Pauli JR, Araujo EP, Moraes JC, de Souza CT, Milanski M, Morari J, Gambero A, Saad MJ, Velloso LA. Interleukin-10 is a protective factor against diet-induced insulin resistance in liver. J Hepatol 2008;48: 628–637
52. Ishizaka S, Saito S, Yoshikawa M, Kimoto M, Nishiyama T. IL-10 production in mouse hepatocytes augmented by TGF-beta. Cytokine 1996;8:837–843
53. Moh A, Zhang W, Yu S, Wang J, Xu X, Li J, Fu XY. STAT3 sensitizes insulin signaling by negatively regulating glycogen synthase kinase-3 β. Diabetes 2008;57:1227–1235
54. Kamada Y, Takehara T, Hayashi N. Adipocytokines and liver disease. J Gastroenterol 2008;43:811–822
55. Kravitz MS, Pitashny M, Shoenfeld Y. Protective molecules: C-reactive protein (CRP), SAP, pentraxin3 (PTX3), mannose-binding lectin (MBL), and apolipoprotein A1 (Apo A1), and their autoantibodies: prevalence and clinical significance in autoimmunity. J Clin Immunol 2005;25:582–591